Maximum Power Generation Control of a Hybrid Wind Turbine Transmission System Based on H∞ Loop-Shaping Approach

Xiuxing Yin[1], Xin Tong[1], Xiaowei Zhao[1] and Aris Karcanias[2]

***Abstract*—The paper presents the design, modelling and optimal power generation control of a large hybrid wind turbine transmission system that seamless integrates planetary/parallel gear sets with a hydraulic transmission to improve the turbine's reliability and efficiency. The hybrid wind turbine has power splitting flows including both mechanical and hydraulic power transmissions. The turbine transmission ratio can be controlled to continuously vary for the maximum wind power extraction and grid integration. Dynamics of the hybrid wind turbine is modeled as an incremental disturbed state space model based on the dynamic equations of each mechanical/hydraulic element. To achieve good tracking and robustness performance, an optimal H∞ loop-shaping pressure controller is designed, which accurately tracks the optimal load pressure in the hydraulic transmission for maximizing wind power generations. The validations of the proposed hybrid wind turbine and the H∞ loop-shaping pressure controller are performed based on a detailed aero-hydro-servo-elastic hybrid type wind turbine simulation platform with both mechanical geared transmission and hydraulic transmission, which is adapted from the NREL (National Renewable Energy Laboratory) 5 MW monopile wind turbine model within FAST (Fatigue, Aerodynamics, Structures, and Turbulence) code. The validation results demonstrate that the hybrid wind turbine achieves better performance in both the maximum wind power extraction and power quality than the hydrostatic wind turbine. In addition, the proposed H∞ loop-shaping pressure controller has better tracking performance than the traditional proportional integral (PI) controller.**

***Index Terms*—Wind turbine; Hybrid transmission; Dynamics modelling; Maximum wind power generation; H∞ loop-shaping control.**

I. INTRODUCTION

A. Background

HISTORICALLY, the geared transmission has been the weakest link in a modern utility scale wind turbine [1]. The failure rates of the gearboxes may be traced to the random gusting nature of the wind and can significantly increase the operating and maintenance costs. On the other hand, the gearless direct-drive wind turbine generators require large amounts of earth magnets (which are rare and expensive), leading to largely increased manufacturing costs. In addition, the direct coupling between the turbine rotor and the electrical generator in a direct-drive wind turbine also causes large misalignment of the drivetrain and significant variations of output voltage and frequency, due to wind gusts and turbulences [2]. Moreover both types of wind turbines mentioned above use fixed ratio transmissions, which therefore require power converters (expensive and fragile) for grid integration.

B. Hydraulic Transmission Based Wind Turbines

As a promising alternative to the above wind turbines, hydraulic transmission based wind turbines have the potential to overcome their shortcomings [3]. The hydraulic transmission can be varied continuously through an infinite number of ratios and this gearing flexibility enables the wind turbine to operate at a more ideal tip speed ratio and thus to enhance the power generation efficiency and cost effectiveness. The hydraulic transmission based wind turbine commonly employs a hydraulic pump driven by the wind turbine rotor and one or more hydraulic motors to transmit the captured wind power [4]. Either the hydraulic pump or the motor has variable displacement. The hydraulic pump converts the mechanical wind energy into pressurized fluid which drives the hydraulic motor. The hydraulic motor is connected to an electrical generator to produce power. The latter can be directly connected to the grid without using power converters, thereby eliminating the common issues associated with converters in grid integrations such as fragility, large harmonics, significant voltage and frequency fluctuations [5]. These harmonics and fluctuations will deteriorate the grid stability and power quality and thus will negatively affect the revenue.

Recently, much attention has been paid to the solutions of hydraulic transmission based wind turbines, ranging from small scaled prototypes up to MegaWatt (MW) scale machines. In [6], a hydraulic wind power system was designed to deliver the wind energy from multiple wind turbines to a centralized generator that runs at a constant speed. A controller was designed and implemented in Simulink and dSPACE 1104 to regulate the flow rate of the system. In [7], piecewise affine models were proposed to approximate a nonlinear hydraulic wind power transfer system. Experimental and simulation studies were conducted to demonstrate the accuracy of the

[1] X. Yin, X. Tong and X Zhao (corresponding author) are with the School of Engineering, the University of Warwick, Coventry, CV4 7AL, U. K. Emails: {x.yin.2, xin.tong, xiaowei.zhao}@warwick.ac.uk.

[2] A. Karcanias is with the FTI Consulting Ltd, 200 Aldersgate, Aldersgate Street, London EC1A 4HD, U. K. Email: aris.karcanias@fticonsulting.com.

This work was funded by the UK Engineering and Physical Sciences Research Council (grant numbers: EP/R007470/1 and EP/R015120/1).

identified model. In [8], a combined method was proposed for wind energy conversion system using pressure coupling hydrostatic transmission. A PID controller and an adaptive fuzzy sliding mode controller were designed to control the generator speed. Experiments were carried out to verify those methods.

A mathematical model of a hydraulic wind power transfer system was presented in [9]. The flow response, angular velocity, and pressure of the system obtained from the mathematical model were compared with experiment test results to evaluate the modelling accuracy. In [10], a dynamic model and a parametric study on the dynamic behavior of a hydraulic wind turbine were presented. A pressure control strategy was proposed to drive a fixed speed generator. In [11], the dynamics of different hydraulic elements in a hydraulic wind power system were studied by taking into account various nonlinearities and pressure dynamics. Consequently, a nonlinear state-space model of the system was derived which was evaluated against experimental data. In [12], a nonlinear model of a hydraulic wind power system at low speed was introduced. Nonlinear state-space representation of the hydraulic wind energy transfer was then presented and validated by experiment. The performance of a multi-MW wind turbine with a hydrostatic transmission was analyzed in [13], which considered the model of each single component, from the blades to the power grid. The analysis model was then used to calculate the annual energy production for different hydrostatic drivetrain configurations.

However, hydraulic wind power systems commonly have relatively low transmission efficiency. In addition since the wind turbine generates a large torque at a relatively low angular velocity, a large displacement hydraulic pump/motor is required for the large volume of the high-pressure hydraulics to transfer the power to the generator. The dependence of hydraulic wind turbines on large displacement hydraulic machines has impeded its widespread deployment in industry. The typical MW scale utility wind turbine operates around 10 rpm and has wind torque input around 1 MNm, which needs the displacement of the hydraulic pump or motor to be designed around 0.02 m^3 for a significantly high hydraulic pressure of 50 MPa. This design seems not very viable since the maximum available pump/motor displacement is around 0.001 m^3 and the 50 MPa pressure is extremely high which is therefore very dangerous for a hydraulic system.

C. Hybrid Transmission Based Wind Turbine

Hence, for multi-MW scale wind turbines, it appears that a hybrid transmission design including both geared and hydraulic transmissions becomes a more feasible option to deal with the challenges of tight size and extremely high pressure met in hydraulic wind turbines. The hybrid transmission wind turbine is constructed by seamlessly incorporating hydraulic transmission with planetary/ parallel gear sets and thus inherits the merits of both systems such as continuously variable operations, reliability, and high efficiency. Since the captured wind power in a hybrid wind turbine is divided into both hydraulic and mechanical power flows, the size and pressure of its hydraulic transmission section can be significantly reduced with increased reliability and efficiency as compared with a pure hydraulic wind turbine. This advantage may become more apparent in offshore which is more suitable for very large wind turbine to be built.

There are relatively few works in the literature focusing on the hybrid transmission based wind turbines. The University of Minnesota designed a hydro-mechanical wind turbine by combining hydraulic transmission with a planetary geared transmission [14]. The turbine transmission ratio can be continuously varied by regulating the hydraulic transmission. However, the dynamics and control design of the turbine were not investigated. In [15], a hydro-mechanical wind turbine was designed by using a hydraulic transmission coupled in series with a single-stage gear set. However, this design is not a real hybrid transmission by nature since the captured wind turbine power is not transmitted through hydraulic and mechanical transmissions in parallel. In [16], a hydro-mechanical wind turbine was designed to improve power generation efficiency by using the support vector regression based optimal predictions of reaction torque. However, the dynamics and control methods were not presented in details.

D. Proposed Work and Contributions

The present paper aims to design a new and large-scale hybrid wind turbine, which incorporates hydraulic transmission with planetary/ parallel gear sets to achieve a more efficient and continuously variable speed transmission system, see Figure 1. The planetary gear set functions as a power splitting mechanism to split the wind power into the hydraulic power and mechanical power. By varying the hydraulic motor displacement in the hydraulic transmission, the continuously variable speed operations can be readily achieved for the maximum wind power extraction of the hybrid wind turbine when the wind is below rated. At this operation region, the turbine blades are kept at an ideal tip speed ratio to provide the maximum aerodynamic efficiency. We mention that the principle of the pitch angle control of the hybrid wind turbine is the same as the conventional wind turbine as their pitch actuation systems are the same.

In this paper, the dynamic equation of the hybrid turbine is derived by combining the dynamic equations of each component including the planetary transmission, the hydraulic transmission, and the electric generator. The dynamic model also considers fluid inertia, compressibility, and flexible long-length high-pressure pipes/hoses effects. The equations of the model are given in an incremental linear state–space representation at the steady state operating point assuming that it has a finite number of modes.

Based on the derived state–space representation, the maximum power generation control of the hybrid wind turbine is equivalent to the optimal tracking control of the load pressure by varying the hydraulic motor displacement. To achieve this aim, a H∞ loop-shaping pressure controller is designed in order to accurately track the optimal load pressure while preserving closed-loop robust stability against external disturbances. The tests of the proposed hybrid wind turbine and the H∞

loop-shaping pressure control system are conducted based on a detailed 5 MW hybrid type wind turbine simulation platform, which is adapted from the NREL 5 MW monopile wind turbine model within FAST code. It is benchmarked against a hydrostatic one which further shows the advantages of hybrid wind turbine. The proposed H∞ loop-shaping pressure controller is also compared with the conventional PI controller, which demonstrates its advantage.

The main novelty and contributions of this paper are highlighted as follows:

(a) The design, modelling and analysis of a large scale hybrid wind turbine by incorporating hydraulic transmission with planetary/ parallel gear sets to achieve a more efficient and continuously variable speed transmission system.

(b) The H∞ loop-shaping pressure control design for the maximum power generation of the hybrid turbine.

(c) The transformation of the NREL 5 MW monopile wind turbine model within FAST code into a hybrid wind turbine as well as comparison and analysis results against a hydrostatic one.

Following this introduction, the paper is structured as follows. Section II presents the design and analysis of the large scale hybrid wind turbine. Section III presents the dynamics modelling and an incremental linear state–space representation of the hybrid turbine. Section IV presents the maximum wind power generation control principle of the hybrid wind turbine. Section V presents the H∞ loop-shaping control design. Section VI presents the verifications and discussions of the hybrid wind turbine within FAST.

II. The Hybrid Wind Turbine

As illustrated in Fig. 1, the proposed hybrid wind turbine mainly consists of a turbine rotor, a planetary gear set, a parallel gear set, a hydraulic transmission, a permanent magnet synchronous generator (PMSG), and necessary mechanical shafts/bearings. The turbine rotor is directly coupled to the planet carrier of the planetary gear set to transfer the captured wind energy into mechanical power of the geared transmission. The planetary gear set functions as a power splitting mechanism to split the wind power into the hydraulic and mechanical powers.

The hydraulic transmission mainly includes a hydraulic pump, a hydraulic motor, pipelines and other necessary accessories including hydraulic accumulator, check valves, and pressure relief valves (not shown in Fig. 1). The fixed displacement hydraulic pump, connected to the ring gear of the planetary gear set via a gear ratio i_p, generates a large flow rate to drive a variable displacement hydraulic motor, which is connected to the sun gear via gear ratio i_m and coupled to the PMSG for electrical power generation. The turbine transmission ratio can be continuously varied as a monotonic function of the motor volumetric displacement. This allows eliminating the fragile power converter that is needed in conventional wind turbines. The hydraulic transmission will absorb wind power oscillations due to wind gusts rather than transmit them through the drivetrain, hence reducing maintenance costs. On the other hand the existence of the gears in the hybrid turbine largely increases the overall efficiency compared with a pure hydraulic transmission wind turbine. In addition, the energy storage component (hydraulic accumulator) of the hybrid turbine can be allocated in the turbine tower or the bottom.

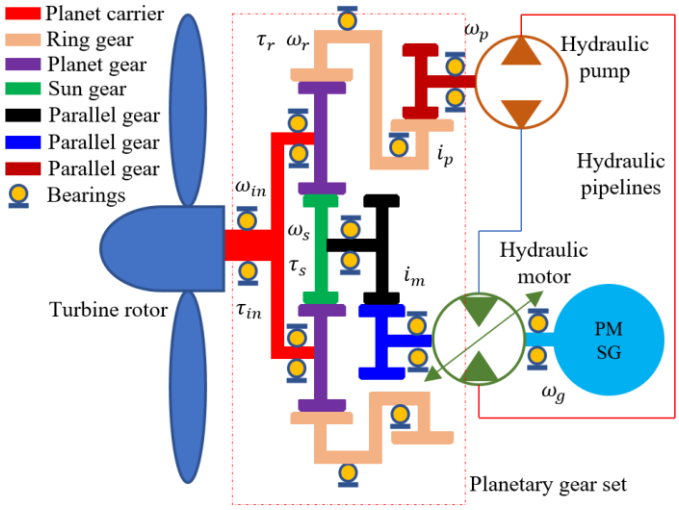

Fig. 1 Schematic of the hybrid wind turbine system

All the above indicate that the hybrid wind turbine has the potential to significantly reduce the weight of the nacelle, enhance reliability and service life of the wind turbine, and reduce its maintenance costs. Thus it is clear that the hybrid transmission has great potential used in the next generation of large wind turbines. It can also be readily achieved by retrofitting existing mechanical geared wind turbines, enabling old-fashioned or inoperative wind turbines to be upgraded.

III. Dynamics Modelling

The dynamic equation of the hybrid turbine system can be derived by combining the dynamic equation of each component including the planetary transmission, the hydraulic transmission, and the electric generator.

A. Dynamics of the Planetary Transmission

The rotational speed relationship of this planetary gear set is

$$(1+k)\omega_{in} = \omega_s - k\omega_r \tag{1}$$

where ω_{in}, ω_s, and ω_r denote the rotational speeds of the turbine rotor, the planetary sun gear, and the planetary ring gear, respectively, k is a constant characteristic coefficient.

The torque relationship is described as

$$\tau_{in} : \tau_r : \tau_s = (1+k) : k : 1 \tag{2}$$

where τ_{in}, τ_r, and τ_s denote the torques of the turbine rotor, the planetary ring gear, and the planetary sun gear, respectively.

The hydraulic pump and rotor speeds are related to the planetary gear set as follows

$$\begin{cases} \omega_p = i_p \omega_r \\ \omega_g = i_m \omega_s \end{cases} \tag{3}$$

where ω_p and ω_g denote the rotational speeds of the hydraulic pump and motor/generator, respectively, i_p and i_m denote the gear ratios of the parallel gear sets that are respectively connected to the hydraulic pump and motor.

Hence, based on (2), the driving torque τ_p for the hydraulic pump can be expressed as

$$\tau_p = \frac{\tau_r}{i_p} = \frac{k}{(1+k)i_p}\tau_{in} \tag{4}$$

B. Dynamics of the Hydraulic Transmission

The hydraulic transmission is designed based on the closed loop hydraulic pump and motor system that is the preferred power element with relatively high operating efficiency (the maximum operating efficiency can approach 90% in practice) [17]. The dynamics of the hydraulic pump and the associated parallel gear set is formulated as

$$\tau_p - D_p P_p - C_r \omega_p = J_p \dot{\omega}_p \tag{5}$$

where D_p and P_p denote the variable pump displacement and the load pressure at the hydraulic pump side, C_r and J_p are viscous damping coefficient and the inertia of the hydraulic pump, respectively. The continuity equation of the hydraulic pump controlled system is expressed as

$$Q_p = D_p \omega_p - C_p P_p \tag{6}$$

where Q_p and C_p are the flow rate and leakage coefficient.

The flowrate of the hydraulic motor is described as

$$Q_m = C_m P_m + D_m \omega_g + \frac{V_o}{\beta_e}\dot{P}_m \tag{7}$$

where C_m and P_m are leakage coefficient and pressure respectively, D_m is the constant displacement, V_o and β_e are respectively the total pressurized volume and the effective bulk modulus.

In practice, flexible long-length high-pressure pipes/hoses are employed to connect the hydraulic pump to the piping toward the hydraulic motor unit. In order to describe the dynamics of the pipelines connecting the hydraulic pump and motor, a state space form is designed to represent the dynamics of the pressure and volumetric flow rates at the hydraulic pump and motor sides of the pipelines [18].

$$\begin{cases} \dot{\boldsymbol{x}}_p = \boldsymbol{A}_p \boldsymbol{x}_p + \boldsymbol{B}_p \boldsymbol{Q} \\ \boldsymbol{P} = \boldsymbol{C}_p \boldsymbol{x}_p \end{cases} \tag{8}$$

where $\boldsymbol{x}_p$, $\boldsymbol{Q}$ and $\boldsymbol{P}$ are the state, input and output respectively. The matrices $\boldsymbol{A}_p, \boldsymbol{B}_p, \boldsymbol{C}_p$ are defined in terms of the physical parameters of the hydraulic pipelines. For the high pressure oil pipeline between the pump and motor, the following vectors are used.

$$\begin{cases} \boldsymbol{Q} = \begin{bmatrix} Q_p & Q_m \end{bmatrix}^{\mathrm{T}} \\ \boldsymbol{P} = \begin{bmatrix} P_p & P_m \end{bmatrix}^{\mathrm{T}} \\ \boldsymbol{x}_p = \begin{bmatrix} p_0 & r_1 & p_1 .... & r_n & p_n \end{bmatrix}^{\mathrm{T}} \\ \boldsymbol{A}_p = \mathrm{diag}\left(0 \ \boldsymbol{A}_{p1} \ \boldsymbol{A}_{p2} .... \ \boldsymbol{A}_{pn}\right) \\ \boldsymbol{B}_p = [\boldsymbol{B}_{pa} \ \boldsymbol{B}_{pb}] = \begin{bmatrix} \boldsymbol{B}_{p0} & \boldsymbol{B}_{p1} ..... \boldsymbol{B}_{pn} \end{bmatrix}^{\mathrm{T}}_{(2n+1)\times 2} \\ \boldsymbol{C}_p = \begin{bmatrix} \boldsymbol{C}_{p1} \\ \boldsymbol{C}_{p2} \end{bmatrix} = \begin{bmatrix} 1 & 0 & 1 & 0 & 1 & 0 & .. \\ 1 & 0 & -1 & 0 & 1 & 0 & .. \end{bmatrix}_{2\times(2n+1)} \end{cases} \tag{9}$$

Assuming the mode number of the fluid transmission line model n=4, the pipeline dynamics is approximated for control design. The detailed parameter values of the above model can be found in [19].

By combing the hydraulic pump/motor flow rate equations with the pipeline state space model, one obtains

$$\begin{aligned} \dot{\boldsymbol{x}}_p &= \boldsymbol{A}_p \boldsymbol{x}_p + \boldsymbol{B}_{pa} \boldsymbol{Q}_p + \boldsymbol{B}_{pb} \boldsymbol{Q}_m \\ &= \boldsymbol{A}_p \boldsymbol{x}_p + \boldsymbol{B}_{pa}\left(D_p \omega_p - C_p \boldsymbol{C}_{p1} \boldsymbol{x}_p\right) + \boldsymbol{B}_{pb} \boldsymbol{Q}_m \\ &= D_p \boldsymbol{B}_{pa} \omega_p + \left(\boldsymbol{A}_p - C_p \boldsymbol{B}_{pa} \boldsymbol{C}_{p1}\right) \boldsymbol{x}_p + \boldsymbol{B}_{pb} \boldsymbol{Q}_m \end{aligned} \tag{10}$$

The dynamics of the (variable displacement) hydraulic motor driven generator system is expressed as

$$D_m P_m - C_g \omega_g - \tau_g = J_g \dot{\omega}_g \tag{11}$$

where C_g and J_g are viscous damping coefficient and total inertia of the hydraulic motor driven generator system, respectively, τ_g is the generator torque.

The dynamics of the hydraulic motor displacement regulation system is modelled as

$$D_{mr} = \zeta_m \dot{D}_m + D_m \tag{12}$$

where D_{mr} and ζ_m are respectively the displacement command and time constant of the hydraulic motor.

C. Dynamics of the Electric Generator

The generator dynamic is generally much faster than the hydraulic transmission system and thus is represented as

$$\tau_{gr} = \zeta_g \dot{\tau}_g + \tau_g \tag{13}$$

where τ_{gr} and ζ_g are respectively the displacement command and time constant for the generator.

D. The Hybrid Turbine Dynamics

The input aerodynamic torque τ_{in} is generally a nonlinear function of the incoming effective wind speed V and turbine rotor speed ω_{in} (when the wind speed is below rated where the pitch angle is usually fixed at a constant value of zero for maximizing wind power generations.) The aerodynamic torque τ_{in} is represented as

$$\tau_{in} = f_{\omega_{in}} \cdot \omega_{in} + f_V \cdot V \tag{14}$$

where $f_{\omega_{in}}$ and f_V are individual partial derivatives and can be derived through FAST linearization at a steady operating point [20].

By combining (1), (3), (4) and (14), the driving torque τ_p for the hydraulic pump is represented as

$$\tau_p = -\frac{k^2 \cdot f_{\omega_{in}}}{(1+k)^2 i_p^2}\omega_p + \frac{k \cdot f_{\omega_{in}}}{(1+k)^2 i_p i_m}\omega_g + \frac{k \cdot f_V}{(1+k) i_p}V \tag{15}$$

By combining (5)-(15), an incremental linear state space model for the hybrid wind turbine system is obtained as

$$\begin{cases} \dot{\hat{\boldsymbol{x}}} = \boldsymbol{A}\hat{\boldsymbol{x}} + \boldsymbol{B}_1\hat{\boldsymbol{u}} + \boldsymbol{B}_2\hat{D} \\ \hat{P}_p = \boldsymbol{C}\hat{\boldsymbol{x}} \end{cases} \tag{16}$$

where $\hat{\boldsymbol{x}} = \boldsymbol{x} - \bar{\boldsymbol{x}}$, $\hat{\boldsymbol{u}} = \boldsymbol{u} - \bar{\boldsymbol{u}}$, $\hat{D} = D - \bar{D}$, $\hat{P}_p = P_p - \bar{P}_p$ denote the incremental states, control input, system disturbances, and control output, respectively.

$\boldsymbol{x} = \left[\omega_p, \boldsymbol{x}_p, P_m, \omega_g, \tau_g, D_m\right]^{\mathrm{T}}$, $\boldsymbol{u} = D_{mr}, D = \left[V, Q_m, \tau_{gr}\right]^{\mathrm{T}}$, $\bar{\boldsymbol{x}}$, $\bar{\boldsymbol{u}}$, $\bar{D}$ and $\bar{P}_p$ denote the steady values of the state variables, control input, system disturbance and control output at the steady state operating point.

The matrices in (16) are represented as

$$\boldsymbol{A} = \begin{bmatrix} -\frac{k^2 \cdot f_{\omega_{in}}}{J_p(1+k)^2 i_p^2} - \frac{C_r}{J_p} & -\frac{D_p \boldsymbol{C}_{p1}}{J_p} & 0 & \frac{k \cdot f_{\omega_{in}}}{J_p(1+k)^2 i_p i_m} & 0 & 0 \\ D_p \boldsymbol{B}_{pa} & \left(\boldsymbol{A}_p - C_p \boldsymbol{B}_{pa}\boldsymbol{C}_{p1}\right) & 0 & 0 & 0 & 0 \\ 0 & -\frac{\beta_e C_m \boldsymbol{C}_{p2}}{V_o} & 0 & -\frac{\beta_e D_m}{V_o} & 0 & 0 \\ 0 & \boldsymbol{0} & \frac{D_m}{J_g} & -\frac{C_g}{J_g} & -\frac{1}{J_g} & 0 \\ 0 & \boldsymbol{0} & 0 & 0 & -\frac{1}{\zeta_g} & 0 \\ 0 & \boldsymbol{0} & 0 & 0 & 0 & -\frac{1}{\zeta_m} \end{bmatrix}$$

$$\boldsymbol{B}_1 = \begin{bmatrix} 0 \\ 0 \\ 0 \\ 0 \\ \frac{1}{\zeta_m} \end{bmatrix}, \quad \boldsymbol{B}_2 = \begin{bmatrix} \frac{k \cdot f_V}{J_p(1+k) i_p} & 0 & 0 \\ 0 & \boldsymbol{B}_{pb} & 0 \\ 0 & 0 & 0 \\ 0 & 0 & 0 \\ 0 & 0 & \frac{1}{\zeta_g} \\ 0 & 0 & 0 \end{bmatrix}, \quad \boldsymbol{C} = \begin{bmatrix} \boldsymbol{0} \\ \boldsymbol{C}_{p1} \\ \boldsymbol{0} \\ \boldsymbol{0} \\ \boldsymbol{0} \\ \boldsymbol{0} \end{bmatrix}^{\mathrm{T}}.$$

where T denotes the transpose operation.

The dynamic modelling of the planetary transmission presented in section III-A is a novel contribution of this paper, which allows establishing the hybrid wind turbine dynamics. The state-space representation (16) of the hybrid wind turbine relates the pressure differential across the hydraulic transmission and the turbine torque/speed to the hydraulic pump displacement. A proper setting of the hydraulic pump displacement allows to optimally control the rotational speed and torque of the turbine rotor. Hence (16) is also a novel contribution that paves the way to conduct the H∞ loop-shaping control design for the maximum wind power generation of the hybrid wind turbine in the following sections.

IV. Maximum Wind Power Generation

Under the rated wind speed, the hybrid wind turbine system is controlled to maximize wind power generations. This is readily achievable by tracking the optimal driving torque τ_{p_opt} of the hydraulic pump. It can be fulfilled by tracking the optimal load pressure P_{p_opt} at the hydraulic pump side as indicated in (4) and (5), which is achievable by continuously adjusting the hydraulic motor displacement D_{mr} as indicated in (16).

At the maximum wind power generation points, the optimal input torque τ_{in_opt} is represented as [21]

$$\tau_{in\_opt} = k_{opt}\omega_{in}^2 \tag{17}$$

where k_{opt} is an optimal constant gain that corresponds to the optimal tip speed ratio at the maximum power tracking points.

Based on (4), the optimal driving torque for the hydraulic pump is

$$\tau_{p\_opt} = \frac{k \cdot k_{opt}\omega_{in}^2}{(1+k) i_p} \tag{18}$$

The turbine rotor speed ω_{in} is readily attainable by measuring the pump and generator speeds based on (1) and (3):

$$\omega_{in} = \frac{\omega_g i_p - k\omega_p i_m}{(1+k) i_p i_m} \tag{19}$$

Therefore, the optimal load pressure P_{p_opt} is derived based on (5) and (18) as follows

$$P_{p\_opt} = \frac{k \cdot k_{opt}\omega_{in}^2}{(1+k) i_p D_p} - \frac{C_r\omega_p + J_p\dot{\omega}_p}{D_p} \tag{20}$$

The optimal load pressure P_{p_opt} can be obtained based on (19) and (20) and can thus be used as the reference input for designing a pressure tracking controller based on (16).

V. H∞ Loop-Shaping Control Design

As illustrated in section IV, the maximum power generation control of this hybrid wind turbine is equivalent to the tracking control of the optimal load pressure P_{p_opt} by varying the hydraulic motor displacement. To achieve this task, a H∞ loop-shaping pressure controller is designed based on the state space model (16). It can guarantee closed-loop stability and robustness and is also particularly suitable for dealing with disturbed complex systems with large amount of state variables [22].

For the wind turbine model (16), the controller is synthesized in the normalized coprime factor form [23]. We denote the transfer function from D_{mr} to $\hat{P}_p$ by G with the state-space realization $(\boldsymbol{A}, \boldsymbol{B}_1, \boldsymbol{C}, 0)$. In order to obtain the desired open loop shape for the controller design, two weighting functions, a pre-compensator W_{pre} and a post-compensator W_{pos} are specified to shape the singular values of the open-loop transfer function. The shaped loop transfer function G_s is

$$G_s = W_{pos} G W_{pre} \tag{21}$$

The pre-compensator W_{pre} is selected to achieve good tracking and disturbance rejection in a low frequency range, while the post-compensator W_{pos} is selected to achieve good robust stability and noise rejection in a high frequency range. In

practice, W_{pre} is selected as an integral action weighting function to make a zero steady state error, while W_{pos} is selected as an identity as listed below

$$\begin{cases} W_{pre} = K_w \dfrac{s+\alpha}{s+\delta}; \\ W_{pos} = 1. \end{cases} \tag{22}$$

where K_w, α and δ are positive constants. δ is selected as a small constant to achieve integral function.

The shaped transfer function G_s is then formulated as a normalized coprime factor with a normalized nominator N_s and denominator M_s factors. Thus,

$$\begin{cases} G_s = \left(N_s + \Delta_{N_s}\right)\left(M_s + \Delta_{M_s}\right)^{-1}; \\ \left\|\Delta_{N_s}, \Delta_{M_s}\right\| \le \varepsilon. \end{cases} \tag{23}$$

where $\Delta_{N_s}, \Delta_{M_s}$ are respectively uncertainty transfer functions in nominator and denominator factors, ε is a stability margin.

The stability margin ε reflects the performance of a controller K_∞ that should be synthesized to satisfy

$$\left\| \begin{bmatrix} I \\ K_\infty \end{bmatrix} \left(I + G_s K_\infty\right)^{-1} \begin{bmatrix} I & G_s \end{bmatrix} \right\|_\infty \le \varepsilon^{-1} \tag{24}$$

By solving the optimization problem in (24), the controller K_∞ can be readily attainable. The optimization problem in (24) is used to ensure the closed-loop stability and can be solved by using the functions *hinfric*, *hinflmi* or *hinfmix* in MATLAB.

Therefore, the H∞ loop shaping controller K is designed as

$$K = W_{pre} K_\infty W_{pos} \tag{25}$$

As indicated in (25), the H∞ loop shaping controller is synthesized by combining the weighting functions W_{pre}, W_{pos} and the controller K_∞ solved in (24). It can be solved by using MATLAB function *loopsyn*.

VI. Verifications and Discussions

The effectiveness tests of the proposed hybrid wind turbine and the H∞ loop-shaping pressure controller were based on a detailed aero-hydro-servo-elastic hybrid wind turbine simulation platform with both mechanical geared transmission and hydraulic transmission, which is transformed from the NREL 5 MW monopile wind turbine model within FAST code.

The FAST code includes higher fidelity turbine structural models with complete nonlinear aerodynamic motion equations and can thus provide an in-depth insight and tremendous flexibility in the control implementations of the hybrid wind turbine. The model simulations provide useful insights into the hydrodynamics and performance predictions of the hybrid wind turbine and are hence mainly utilized to evaluate the maximum power extraction control of the hybrid wind turbine system under the rated wind speed of 12 m/s.

In order to transform the baseline NREL 5 MW geared transmission wind turbine into a 5 MW hybrid type wind turbine, the ElastoDyn input file of FAST was modified to only enable the generator DOF (degree of freedom) and disenable the turbine structural information such as the drivetrain torsional flexibility DOF such that the 5 MW wind turbine operates with a rigid drivetrain shaft. Then, the geared transmission ratio of the baseline wind turbine was changed to $\left(1+k\right)i_p/k$ in the hybrid wind turbine and the generator in the baseline wind turbine was regarded as the hydraulic pump in the hybrid wind turbine such that the two turbines have equivalent dynamics equations in the FAST. The hybrid wind turbine was implemented into FAST by using an interface between MATLAB/Simulink and FAST as shown in Fig. 2.

The hybrid wind turbine model was constructed based on (1)-(16) and the H∞ loop-shaping pressure controller was designed based on (21)-(25). All of them have been incorporated into the NREL 5-MW wind turbine model to obtain a hybrid wind turbine in Fig. 2. The designed pitch angle controller in Fig. 2 is a gain-scheduled PI controller with the PI gains K_P and K_I scheduled by the pitch angle β:

$$K_p(\beta) = -\frac{1.2933}{1+\dfrac{\beta}{6.3023}}, K_I(\beta) = -\frac{0.5543}{1+\dfrac{\beta}{6.3023}} \tag{26}$$

The above scheduling ensures that the idealized response of the rotor speed error will be like that of a second-order system with the natural frequency of 0.6 rad/s and the damping ratio of 0.7 recommended by Jonkman [25].

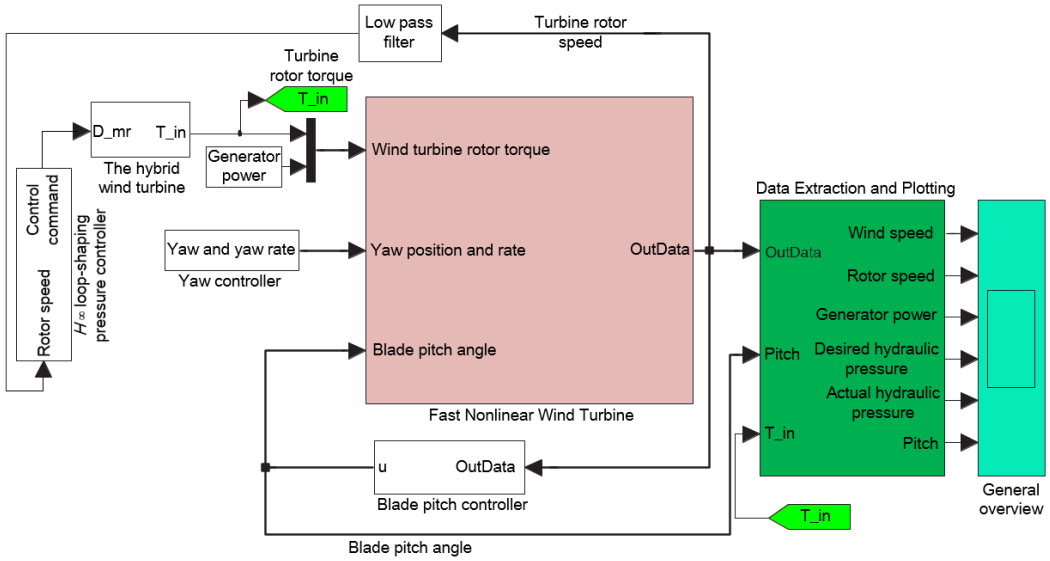

Fig. 2. The implementation of the designed controller in Simulink with FAST wind turbine block

The number of modes for the hydraulic pipeline dynamics was chosen to be 4, which results in a stable 11th-order plant. The shaped loop transfer function G_s was selected as $G_s(s) = \dfrac{4225}{(s+10^{-7})(s+78)}$. Its gain crossover frequency is 46.52 rad/s and the high-frequency roll-off is about -40 dB/decade. After implementing the loop-shaping controller, the closed-loop gain is 1.72, which means that the modelling uncertainties (which are less than the stability margin of 0.58) are tolerated. As shown in Fig. 3, the phase and gain margins of closed loop system are 74.5 deg and 35.1 dB, respectively, and the closed-loop step response has an overshoot of 0 and a settling time of 0.07 s.

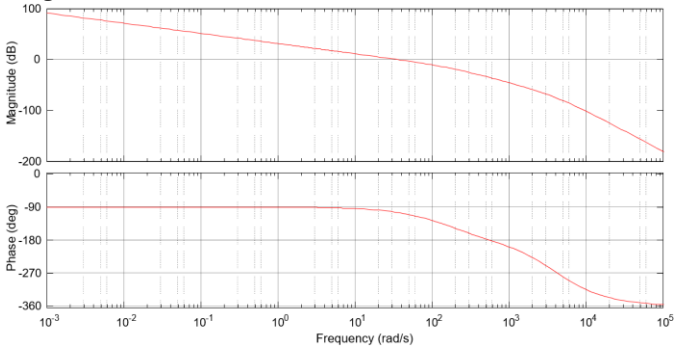

Fig. 3. The Bode plot of the control loop

We now compare the hybrid wind turbine with a counterpart 5 MW hydrostatic wind turbine developed in [26] under the same operating conditions in FAST to further evaluate its superiorities. The main simulation parameters are listed in Table 1. The transformed upwind NREL 5 MW wind turbine has a rotor diameter of 126 m and a hub height of 90 m. During the simulations, the wind turbine operates around the rated rotor speed of 12 rpm in region 2. The steady state operating point for linearizing the nonlinear wind turbine model was set at the wind speed of 9 m/s. The rated generator torque is 43,093 Nm and the maximum generator torque is 47,402 Nm.

TABLE I
THE SIMULATION PARAMETERS

Symbol	Quantity	Values
k	Gear set constant	4
i_p	Pump side parallel transmission ratio	1
i_m	Hydraulic motor side parallel transmission ratio	1
C_r	Pump side viscous damping coefficient	0.03
C_g	Hydraulic motor side damping coefficient	0.02
J_p	Pump side inertia	2000 kg•m^2
C_p	Pump leakage coefficient	10^{-7} m^3/s/Pa
C_m	Hydraulic motor leakage coefficient	10^{-7} m^3/s/Pa
D_m	The hydraulic motor displacement	10^{-6} m^3/rad
V_o	The total pressurized volume	5 m^3
β_e	The effective bulk modulus	5×10^5 N/m^2
J_g	The total inertia of the hydraulic motor and generator	100 kg•m^2
ζ_g	The time constant for generator	1000 s^{-1}
ζ_p	The time constant for the pump	100 s^{-1}
ω_g	The generator speed	1500 rpm

As illustrated in Fig. 4, the input wind speeds are generated by NREL TurbSim with values varying between 3 m/s and 11 m/s. Irregular waves were generated based on the JONSWAP/Pierson-Moskowitz spectrum by the HydroDyn module of FAST.

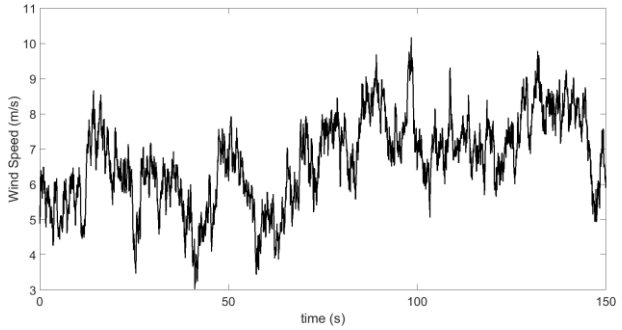

Fig. 4. Wind speed variations

As shown in Fig. 5, the hybrid wind turbine operates at the rotor speed between 9 rpm and 13 rpm, while the hydrostatic wind turbine operates at the rotor speed between 7.5 rpm and 9

rpm. Since the rotor speed of the hybrid wind turbine is more close to the rated rotor speed of 12 rpm than that of the hydrostatic wind turbine, the hybrid wind turbine can generate more power than the hydrostatic wind turbine. In addition, the hydraulic machines (including a hydraulic motor and a pump) of the hybrid wind turbine have much smaller displacements and thus is more easily realized than that in the hydrostatic wind turbine since the turbine rotor speed largely determines the hydraulic machine sizes with the same power rating.

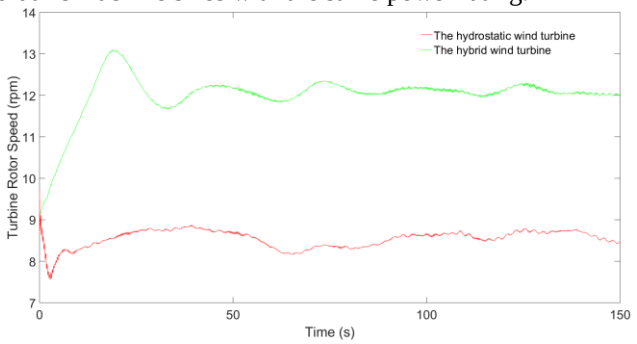

Fig. 5. Wind turbine rotor speed variations

As shown in Figs. 6 and 7, by using the designed H∞ loop-shaping pressure controller, the actual load pressure from the hybrid wind turbine can accurately track the optimal load pressure calculated from (20) corresponding to the maximum wind power extraction points. Therefore, the maximum power generation control of a hybrid wind turbine can be readily achieved based on the proposed H∞ loop-shaping approach.

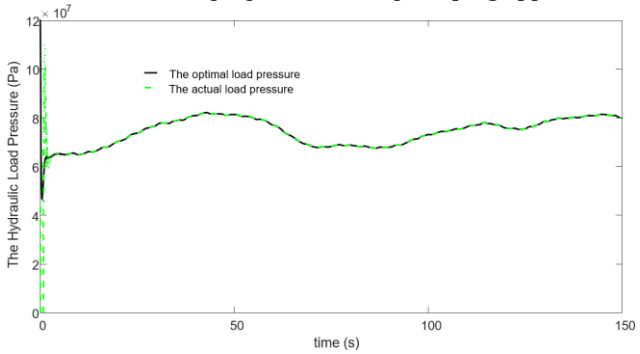

Fig. 6. The hydraulic load pressure variations in 150 s

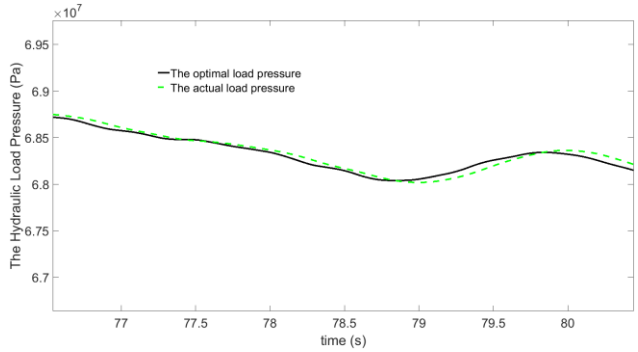

Fig. 7. The hydraulic load pressure variations

As illustrated in Fig. 8, the generator power produced by the hybrid wind turbine is obviously larger than that from the hydrostatic wind turbine. Since the two wind turbines have the same wind power inputs and are controlled by the same type controller, the hybrid wind turbine apparently has higher efficiency than the hydrostatic wind turbine.

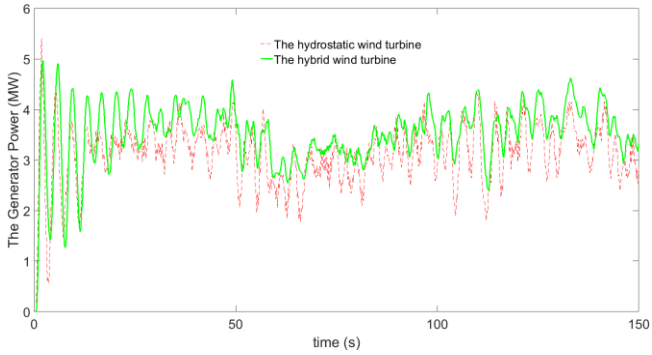

Fig. 8. The generator power variations

In order to further evaluate the performances of the proposed H∞ loop-shaping control approach, it is benchmarked against a traditional proportional integral (PI) controller under a full-field turbulent wind speed inputs from 3 m/s to 25 m/s with large external disturbances. As illustrated in Fig. 9, the optimal hydraulic load pressure is more accurately tracked by using the proposed H∞ loop-shaping controller than using the PI controller whose tracking exhibits some obvious deviations. The mean absolute percentage error (MAPE) and the mean square percentage error (MSPE) [24] of the tracking errors by using the proposed H∞ loop-shaping controller are respectively 1.56×10^{-4} and 8.27×10^{-7}, while they are respectively 8.24×10^{-4} and 1.85×10^{-6} when using the PI controller. Hence, the proposed H∞ loop-shaping controller clearly has better tracking and robust performances against large turbulent wind disturbance inputs, than the PI controller.

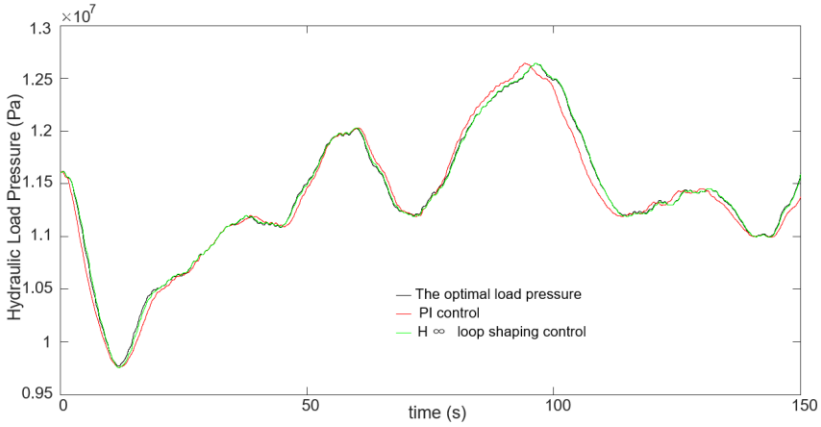

Fig. 9. The hydraulic load pressure variations under the PI control and *H*∞ loop-shaping pressure control

Furthermore, the hybrid wind turbine potentially has relatively lower cost than the traditional geared wind turbine as the mechanical components in the transmission system of the hybrid turbine are much smaller which can be properly controlled as indicated in the above results. And it does not need power converter which is expensive and fragile. In comparison with hydrostatic wind turbine, the cost of the hybrid wind turbine can also be potentially cheaper since the number of large size and high cost hydraulic components in hydrostatic transmission can be significantly reduced in the hybrid wind turbine. In addition, since the hybrid wind turbine has energy storage component - hydraulic accumulator, it has the potential to provide firm frequency response (FFR) service in particularly if a few hybrid turbines share a big accumulator in a wind farm. Of course, the size hydraulic accumulator may need increase if FFR service is planned than only used for the normal operations of the hybrid wind turbine.

VII. Conclusion

This paper has presented the design, dynamic modelling and the maximum power generation control (based on H∞ loop-shaping control approach) of a large hybrid wind turbine. The hybrid wind turbine was constructed by integrating mechanical geared transmission with hydraulic transmission to achieve a more effective continuously variable hybrid transmission operating with a wide speed range. The dynamic model of the hybrid turbine has been derived by combining the dynamic equations of each component and an incremental state-space representation has been derived at the steady state operating point. Consequently, a H∞ loop-shaping pressure controller is designed to extract the maximum wind power by accurately tracking the optimal load pressure. The effectiveness validation of the proposed hybrid wind turbine and the H∞ loop-shaping pressure controller were performed based on a detailed hybrid type wind turbine simulation platform with both mechanical geared transmission and hydraulic transmission, which was transformed from the high fidelity NREL 5 MW monopile wind turbine model within FAST code. The credible model simulation results demonstrate that the hybrid wind turbine can capture much more power than the hydrostatic wind turbine. In addition, the proposed H∞ loop-shaping controller has better load pressure tracking and robust performances against large turbulent wind disturbance inputs than the conventional PI controller. Such results indicate the feasibility of hybrid wind turbines and also shows the superiorities of the H∞ loop-shaping controller over the conventional PI controller.

The proposed hybrid wind turbine system holds many advantages over the mechanical geared or hydrostatic wind turbine systems, such as higher reliability, wider working range of wind speed, quicker response and lower cost. Future work includes building a prototype of the proposed hybrid wind turbine, based on which more benchmark experiments will be conducted to verify the proposed modelling and control approaches.

References

[1] Jiang Z, Yang L, Gao Z, et al. Numerical simulation of a wind turbine with a hydraulic transmission system. Energy Procedia, 2014, 53: 44-55.
[2] Ragheb A M, Ragheb M. Wind turbine gearbox technologies. Fundamental and Advanced Topics in Wind Power. InTech, 2011.
[3] Cai M, Wang Y, Jiao Z, et al. Review of fluid and control technology of hydraulic wind turbines. Frontiers of Mechanical Engineering, 2017, 12(3): 312-320.
[4] Qin C, Innes-Wimsatt E, Loth E. Hydraulic-electric hybrid wind turbines: Tower mass saving and energy storage capacity. Renewable Energy, 2016, 99: 69-79.
[5] S. Yasmeena, G. Tulasiram Das. A Review of Technical Issues for Grid Connected Renewable Energy Sources. International Journal of Energy and Power Engineering. Special Issue: Energy Systems and Developments. 2015, 4, 5-1, 22-32.
[6] Vaezi M, Asgharifard A, Izadian A. Control of Hydraulic Wind Power Transfer System under Wind and Load Disturbances. IEEE Transactions on Industry Applications, 2018.
[7] Vaezi M, Izadian A. Piecewise affine system identification of a hydraulic wind power transfer system. IEEE Transactions on Control Systems Technology, 2015, 23(6): 2077-2086.
[8] Do H T, Dang T D, Truong H V A, et al. Maximum Power Point Tracking and Output Power Control on Pressure Coupling Wind Energy Conversion System. IEEE Trans. on Industrial Electronics, 2018, 65(2): 1316-1324.
[9] Izadian A, Hamzehlouia S, Deldar M, et al. A hydraulic wind power transfer system: Operation and modeling. IEEE Transactions on Sustainable Energy, 2014, 5(2): 457-465.
[10] Laguna A J, Diepeveen N F B, van Wingerden J W. Analysis of dynamics of fluid power drive-trains for variable speed wind turbines: parameter study. IET Renewable Power Generation, 2014, 8(4): 398-410.
[11] Deldar M, Izadian A, Vaezi M, et al. Modeling of a hydraulic wind power transfer utilizing a proportional valve. IEEE Transactions on Industry Applications, 2015, 51(2): 1837-1844.
[12] Vaezi M, Deldar M, Izadian A. Hydraulic Wind Power Plants: A Nonlinear Model of Low Wind Speed Operation. IEEE Transactions on Control Systems Technology, 2016, 24(5): 1696-1704.

[13] Silva P, Giuffrida A, Fergnani N, et al. Performance prediction of a multi-MW wind turbine adopting an advanced hydrostatic transmission. Energy, 2014, 64: 450-461.
[14] F. Wang, B. Trietch, K.A. Stelson, Mid-sized wind turbine with hydro-mechanical transmission demonstrates improved energy production, Proc. 8th International Conference on Fluid Power Transmission and Control (ICFP 2013), Hangzhou, China, 2013.
[15] Lin Y, Tu L, Liu H, et al. Hybrid power transmission technology in a wind turbine generation system. IEEE/ASME Transactions on Mechatronics, 2015, 20(3): 1218-1225.
[16] Shamshirband S, Petković D, Amini A, et al. Support vector regression methodology for wind turbine reaction torque prediction with power-split hydrostatic continuous variable transmission. Energy, 2014, 67: 623-630.
[17] Merritt H E. Hydraulic control systems. John Wiley & Sons, 1967.
[18] Makinen, J., Pertola, P., and Marjamaki, H., 2010, Modeling Coupled Hydraulic-Driven Multibody Systems Using Finite Element Method, 1st Joint International Conference on Multibody System Dynamics, Lappeenranta University of Technology.
[19] Laguna A J. Modeling and analysis of an offshore wind turbine with fluid power transmission for centralized electricity generation. Journal of Computational and Nonlinear dynamics, 2015, 10(4): 041002.
[20] Dana S, Damiani R, vanDam J. Validation of Simplified Load Equations through Loads Measurement and Modeling of a Small Horizontal-Axis Wind Turbine Tower; NREL (National Renewable Energy Laboratory), Golden, CO (United States), 2015.
[21] Kumar D, Chatterjee K. A review of conventional and advanced MPPT algorithms for wind energy systems. Renewable and sustainable energy reviews, 2016, 55: 957-970.
[22] McFarlane D, Glover K. A loop-shaping design procedure using H/sub infinity/synthesis. IEEE trans on automatic control, 1992, 37(6): 759-769.
[23] McFarlane D C, Glover K. Robust controller design using normalized coprime factor plant descriptions. Springer, 1990.
[24] Kusiak A, Zhang Z. Adaptive control of a wind turbine with data mining and swarm intelligence. IEEE Trans on Sustainable Energy, 2011, 2(1): 28-36.
[25] Jonkman J M. Dynamics modeling and loads analysis of an offshore floating wind turbine. 2007.
[26] Tong X, Zhao X. Power generation control of a monopile hydrostatic wind turbine using an loop-shaping torque controller and an LPV pitch controller. IEEE Transactions on Control Systems Technology, 2018, 26 (6): 2165-2172

Xiuxing Yin received his Ph. D. in mechatronic engineering from Zhejiang University, Hangzhou, China in 2016. He is now a research fellow at the University of Warwick, U. K. His research interests focus on mechatronics, renewable energy and nonlinear control.

Xin Tong is a research engineer in Jaguar Land Rover Limited. She obtained her PhD in Engineering in 2017 from the University of Warwick. She obtained her MSc (Distinction) in Control Systems in 2013 from Imperial College London, and obtained her BEng in Electrical Engineering & Automation in 2012 from Huazhong University of Science and Technology. Her current research interest is control of large offshore wind turbines, and powertrain control & calibration.

Xiaowei Zhao is Professor of Control Engineering at the School of Engineering, University of Warwick. He obtained his PhD degree in Control Theory from Imperial College London. After that he worked as a postdoctoral researcher at the University of Oxford for three years before joining Warwick in 2013. His research interests include (1) control of wind/tidal turbines/farms; (2) grid integration of renewable energy; (3) microgrid; (4) control of fluid-structure interaction with applications to large and flexible wind turbines, highly flexible aircraft, and long-span suspension bridges; (5) control of coupled infinite-dimensional systems.

Aris Karcanias is the co-lead of the Global Clean Energy Practice at FTI Consulting. He has a technical engineering background, with extensive experience leading board-level strategy, technology development, and M&A for leading utilities, manufacturers, and investors. Aris specialises in clean energy systems, their integration, and the redesign of the future energy system.